

Distinct adipogenic differentiation phenotypes of human umbilical cord mesenchymal cells dependent on adipogenic conditions

Jessica Saben^{1,2}, Keshari M Thakali^{1,2}, Forrest E Lindsey¹, Ying Zhong¹, Thomas M Badger^{1,2}, Aline Andres¹ and Kartik Shankar^{1,2}

¹Arkansas Children's Nutrition Center, University of Arkansas for Medical Sciences, Little Rock, AR 72202, USA; ²Department of Pediatrics, University of Arkansas for Medical Sciences, Little Rock, AR 72202, USA

Corresponding author: Kartik Shankar. Email: ShankarKartik@uams.edu

Abstract

The umbilical cord (UC) matrix is a source of multipotent mesenchymal stem cells (MSCs) that have adipogenic potential and thus can be a model to study adipogenesis. However, existing variability in adipocytic differentiation outcomes may be due to discrepancies in methods utilized for adipogenic differentiation. Additionally, functional characterization of UCMSCs as adipocytes has not been described. We tested the potential of three well-established adipogenic cocktails containing IBMX, dexamethasone, and insulin (MDI) plus indomethacin (MDI-I) or rosiglitazone (MDI-R) to stimulate adipocyte differentiation in UCMSCs. MDI, MDI-I, and MDI-R treatment significantly increased peroxisome proliferator-activated receptor gamma (*PPAR* γ) and CCAAT-enhancer binding protein alpha (*C/EBP* α) mRNA and induced lipid droplet formation. However, MDI-I had the greatest impact on mRNA expression of *PPAR* γ , *C/EBP* α , *FABP4*, *GPD1*, *PLIN1*, *PLIN2*, and *ADIPOQ* and lipid accumulation, whereas MDI showed the least. Interestingly, there were no treatment group differences in the amount of *PPAR* γ protein. However, MDI-I treated cells had significantly more *C/EBP* α protein compared to MDI or MDI-R, suggesting that indomethacin-dependent increased *C/EBP* α may contribute to the adipogenesis-inducing potency of MDI-I. Additionally, bone morphogenetic protein 4 (BMP4) treatment of UCMSCs did not enhance responsiveness to MDI-induced differentiation. Finally to characterize adipocyte function, differentiated UCMSCs were stimulated with insulin and downstream signaling was assessed. Differentiated UCMSCs were responsive to insulin at two weeks but showed decreased sensitivity by five weeks following differentiation, suggesting that long-term differentiation may induce insulin resistance. Together, these data indicate that UCMSCs undergo adipogenesis when differentiated in MDI, MDI-I, and MDI-R, however the presence of indomethacin greatly enhances their adipogenic potential beyond that of rosiglitazone. Furthermore, our results suggest that insulin signaling pathways of differentiated UCMSCs are functionally similar to adipocytes.

Keywords: Adipogenesis, mesenchymal stem cells, umbilical cord, peroxisome proliferator-activated receptor gamma, insulin signaling

Experimental Biology and Medicine 2014; **239**: 1340–1351. DOI: 10.1177/1535370214539225

Introduction

The umbilical cord (UC) matrix, also known as Wharton's Jelly, is a potential source of mesenchymal stem cells (MSCs) for clinical and therapeutic applications.^{1,2} UC matrix cells have been characterized to have cell-surface markers typical of MSCs (positive for CD10, CD13, CD29, CD44, CD73, CD90, and CD105 and negative for CD14, CD33, CD56, CD31, CD34, and CD45)^{3–5} and can differentiate into a number of cell types including: dermal fibroblasts,⁶ osteoblasts,^{7,8} chondrocytes,^{7,9} adipocytes,⁷ myocytes,¹⁰ hepatocytes,^{11,12} and neural cells.^{13,14} Furthermore, compared to embryonic stem cells, UCMSCs are a non-controversial

resource of multipotent stem cells that can be obtained in large quantities,^{4,11} and have been shown to retain stem-like qualities over long-term culture.¹⁵ In addition to their importance in tissue engineering, transplanted UCMSCs have recently been shown to provide therapeutic benefits in injured renal¹⁶ and hepatic¹⁷ tissue through the release of exosomes. UCMSCs also provide an easily accessible source of human stem cells that can be utilized to study the mechanisms regulating lineage differentiation. Finally, UCMSCs are likely to provide a unique resource to study the impact of developmental programming in the offspring.

The process of cellular differentiation into adipocytes (*viz.* adipogenesis) has been extensively studied due to the

central role of adipose tissue in disorders such as obesity, type 2 diabetes, and numerous other related metabolic disorders. Obesity develops from a chronic positive energy imbalance, where energy intake exceeds energy expenditure. Throughout development, adipose tissue expansion is regulated by processes of hypertrophy and hyperplasia. Extensive hypertrophy, as often seen with obesity, can induce a metabolically inflexible and hormone-resistant state, driving the metabolic perturbations that accompany obesity.^{18,19} On the other hand, adipose tissue hyperplasia has been shown to help maintain a healthy and metabolically responsive phenotype.¹⁹ The production of new adipocytes through adipogenesis proceeds through a series of finely tuned steps, beginning with commitment of cells to the adipocyte lineage and culminating in terminal differentiation and acquisition of adipocytic phenotype characterized by lipid accumulation.^{20,21} To date, many of the mechanisms regulating adipocyte function and differentiation have been widely examined using the mouse fibroblast-derived preadipocyte cell line, 3T3-L1.^{22–24} Other studies have been carried out using bipotential or multipotential cell lines and primary mesenchymal cells isolated from the bone-marrow. UCMSCs also provide a relatively accessible human *in vitro* system to study adipogenesis and as a source of fetal stem cells, can be used to test the effects of the *in utero* environment on differentiation potential. Several differentiation protocols have been utilized to induce adipogenesis in UCMSCs (reviewed by Scott et al.²⁵), which can result in various phenotypic outcomes and levels of differentiation, indicating a need for studies that compare the outcomes of various differentiation protocols. Most importantly, characterization of the functionality of adipocytes differentiated from UCMSCs has not yet been described. Finally, although markers of terminal adipocyte differentiation have been characterized to some degree in these cells,^{7,26–29} adipocyte commitment has not been explored.

In vitro differentiation of UCMSCs into adipocytes can be achieved by inducing adipogenic transcription factors, peroxisome proliferator-activated receptor gamma (PPAR γ) and CCAAT-enhancer binding proteins (C/EBP α and β),³⁰ with a differentiation cocktail termed MDI. MDI consists of a phosphodiesterase inhibitor (M: 3-isobutyl-1-methylxanthine, IBMX), a glucocorticoid (D: dexamethasone), and insulin (I). In most cases, MDI is supplemented with a cyclooxygenase inhibitor such as indomethacin or a PPAR γ agonist like rosiglitazone. Both indomethacin and rosiglitazone have been shown to induce adipogenesis through the stimulation of PPAR γ .^{31–33} via slightly different mechanisms. Indomethacin drives PPAR γ expression, whereas rosiglitazone, a potent PPAR γ ligand, increases its transcriptional activity.³¹ Furthermore, both chemicals have been shown to induce gene expression changes that are independent of PPAR γ activation^{31,34} that may lead to different levels of differentiation.

There were three main goals in this study to further characterize the adipogenic phenotype of UCMSCs. The first objective was to determine the adipogenic response of UCMSCs to three differentiation conditions: MDI, MDI-indomethacin (MDI-I), and MDI-rosiglitazone (MDI-R) via

analysis of cellular morphology, gene expression, and protein levels. Secondly, we set out to determine if treatment with bone morphogenetic protein 4 (BMP4), a potent inducer of adipocyte commitment in the murine mesenchymal stem cell line C3H10T1/2,³⁵ will commit UCMSCs to an adipocyte lineage, thereby enhancing the differentiation response to MDI, MDI-I, and/or MDI-R. Finally, we aimed to functionally characterize UCMSCs differentiated into adipocytes by testing their responsiveness to insulin challenge. We hypothesized that MDI-I will induce the greatest adipogenic response in UCMSCs, and that exposure to BMP4 will commit all cells to an adipocyte lineage, therefore eliminating the differential effects of the three types of differentiation media.

Materials and methods

Isolation of UCMSCs

All chemicals were purchased from Sigma-Aldrich (St. Louis, MO) unless otherwise specified. UCs were collected at the University of Arkansas for Medical Sciences (UAMS), after obtaining written informed consent from mothers during the first trimester of pregnancy. The protocol was approved by the Institutional Review Board at the University of Arkansas for Medical Sciences (NCT01131117). Three inch pieces of UCs from two patients were washed three times with phosphate-buffered saline (PBS) containing 1% antibiotic-antimycotic (ABAM) (Life Technologies, Carlsbad, CA) and stored at 4°C until processing (within 2–3 h of collection). Cells from the UC matrix (UCMSCs) were isolated from the two UCs, pooled, and expanded using media as described elsewhere.³⁶ In brief, UCs were divided into 1 in pieces, sliced open longitudinally using a sterile surgical blade to expose the UC matrix, vessels were removed, and tissue was scored horizontally many times to help liberate the cells. Next, the tissue underwent a series of enzymatic digestions (300 U/mL collagenase + 1 mg/mL hyaluronidase [45 min], and 0.25% trypsin-ethylene diamine tetraacetic acid [EDTA] [15 min]), followed by 10 min of scraping the tissue with forceps in 1x PBS to remove cells. The solution was placed on a 100 μ m cell strainer; cells were collected, and centrifuged at 1000 r/min for 5 min. UCMSCs were counted and plated in growth media (Supplemental Table 1) in a single well of a six-well plate. Cells were expanded until the third passage after which they were fluorescently labeled with antibodies against CD13, CD29, CD44, CD90, CD105, CD31, CD34, and CD45 (BioLegend, San Diego, CA) and analyzed via FACS. UCMSCs were then plated for adipogenesis experiments described below.

Cell culture and adipocyte differentiation

UCMSCs were maintained in growth media until reaching 80% confluence. Cells were plated for experimentation at 1x 10⁴ cells/cm², one day prior to treatment with BMP4 (R&D Systems, Minneapolis, MN) or vehicle, after which media containing BMP4 (50, 100, 150 ng/mL) or vehicle, which was replaced every other day for four days. UCMSCs were either collected at this point or treated

with adipogenic media: Dulbecco's Modified Eagle's medium (DMEM) containing 10% fetal bovine serum (FBS), 1% ABAM, 1 μ mol/L dexamethasone, 500 μ mol/L IBMX, 1 μ mol/L insulin (MDI) with the addition of either 60 μ mol/L indomethacin (MDI-I), or 10 μ mol/L rosiglitazone (Cayman Chemicals, Boston, MA) (MDI-R). Cells were cultured for up to five weeks with the appropriate adipogenic media replaced every third day. An insulin challenge was performed in some cases on differentiated cells. For these experiments, cells were serum starved for 16 h followed by treatment with 100 nmol/L insulin for 10 min. The insulin was removed, cells washed with PBS, and collected for protein analysis as described below.

mRNA isolation and qRT-PCR

Total RNA was isolated using a RNeasy Mini kit including on-column DNase digestion (Qiagen, Valencia, CA) from $n=6$ replicates per treatment group. RNA integrity was assessed using Experion RNA StdSens analysis kit (BioRad). Total RNA (1 μ g) was reverse transcribed using iScript cDNA synthesis kit (BioRad), and subsequent real-time PCR analysis was performed using an ABI Prism 7500 FAST sequence detection system (Applied Biosystems, Foster City, CA). Gene specific primers were designed using Primer Express Software (Applied Biosystems). The relative amounts of mRNA were quantified using a standard curve and normalized to the expression of *SRP14* mRNA. Primer sequences are depicted in Supplemental Table 2. To confirm that the changes observed following adipogenic differentiation were not unique to the initial UCMSC samples, additional UCMSCs were collected from four more subjects, expanded individually and differentiated as mentioned above. At 0, 2, and 5 weeks after adipogenic differentiation, total RNA was isolated, reverse transcribed and used for real-time PCR analysis as described above.

Oil-red-O staining and microscopy

UCMSCs ($n=3$ replicates per treatment group) were fixed for 15 min in 3% paraformaldehyde, permeabilized with 0.1% Triton X-100 for 5 min, and blocked with PBS containing 5% BSA for 30 min at room temperature. To visualize lipid accumulation over the differentiation time course, cells were stained with a lipid soluble dye (Oil-red-O in 60% isopropanol) for 45 min, followed by three washes with PBS. Actin filaments were stained using Alexa fluor-488 phalloidin (Life Technologies) per manufacturer's instructions. All fluorescent labeling dyes were examined using an Axio Vert 200 fluorescent microscope (Carl Zeiss, Oberkochen, Germany). Axiovision software (Carl Zeiss) was used to semi-quantitatively estimate the amount of triglyceride (TG) storage by measuring the percentage of Oil-red-O staining per 40 \times field and normalizing to nuclear content (count of 4',6-diamidino-2-phenylindole [DAPI]-stained nuclei/field). Lipid droplet size was also semi-quantitatively estimated using Axiovision software, by dividing the total area stained with Oil-red-O in each field by the number of individual particles. Four 40 \times fields were analyzed per sample ($n=3$ replicates per treatment group).

Protein isolation and immunoblotting

Total cell lysates from $n=3-5$ replicates per treatment group were prepared in RIPA buffer (25 mmol/L Tris-HCl, 150 mmol/L NaCl, 1.0% NP-40, 1.0% deoxycholic acid, 0.1% sodium dodecyl sulfate [SDS], 2 mmol/L EDTA) containing 1 mmol/L phenylmethanesulfonyl fluoride (PMSF) and protease inhibitor cocktail. Proteins were resolved by SDS-polyacrylamide gel electrophoresis (PAGE) and immunoblotting was carried out using standard procedures.³⁷ Membranes were incubated with primary antibodies against PPAR γ (#sc-7196), phosphorylated ERK1/2 (P-ERK1/2) (#sc-81492) (both from Santa Cruz Biotechnology Inc., Dallas, TX), C/EBP α (#3087), C/EBP β (#229 C), AKT (#9272), phosphorylated AKT (P-AKT) (#5106S), JNK (#9258), phosphorylated JNK (P-JNK) (#4668), ERK1/2 (#46955), and α -tubulin (#9099S) (Cell Signaling, Danvers, MA) for 16 h at 4 $^{\circ}$ C. horseradish peroxidase (HRP)-conjugated secondary antibodies against rabbit and mouse IgG (Santa Cruz Biotechnology, Inc.) were used for protein detection. Quantitation of immunoblots was performed using Quantity One software (Biorad).

Statistical analysis

Real-time RT-PCR data are expressed as mean fold change from control \pm SEM and all other data are expressed as means \pm SEM. None of the data is transformed. Repeated measures two-way ANOVA followed by Tukey's or Sidak's multiple comparisons test was used to compare the three differentiation treatments across multiple time points. For BMP stimulation of UCMSCs, one-way ANOVA followed by all-pair wise comparison with the Student-Neuman-Keuls method was performed. For all statistical tests, $P \leq 0.05$ was considered to be statistically significant. Statistical analyses were performed using GraphPad Prism 6 (v 6.02, La Jolla, CA).

Results

UC matrix cells express MSC surface markers

Flow cytometric analysis of cell surface antigens revealed that expanded UC cells homogenously expressed CD13, CD29, CD44, CD90, and CD105, whereas only 0.3% of cells expressed CD31, CD34, and CD45 (Figure 1), confirming a MSC phenotype.

MDI-I induces the greatest adipogenic response by five weeks

Adipocyte differentiation is characterized by the establishment of a transcriptional program that drives adipocyte-specific gene expression and function. Consistent with adipocyte differentiation, MDI, MDI-I, and MDI-R treatment led to \sim six-fold and \sim five-fold increase in the expression of adipogenic transcriptional regulators, PPAR γ and C/EBP α , respectively, by one week of treatment ($P < 0.001$, Figure 2a). Additionally, mRNA expression of lipid droplet proteins, *PLIN1* and *PLIN2*, were significantly induced ($P < 0.001$) by 5-fold and 4-fold with MDI, 38-fold and 14-fold with MDI-I, and 105-fold and 12-fold MDI-R, respectively, following one week of differentiation (Figure 2a).

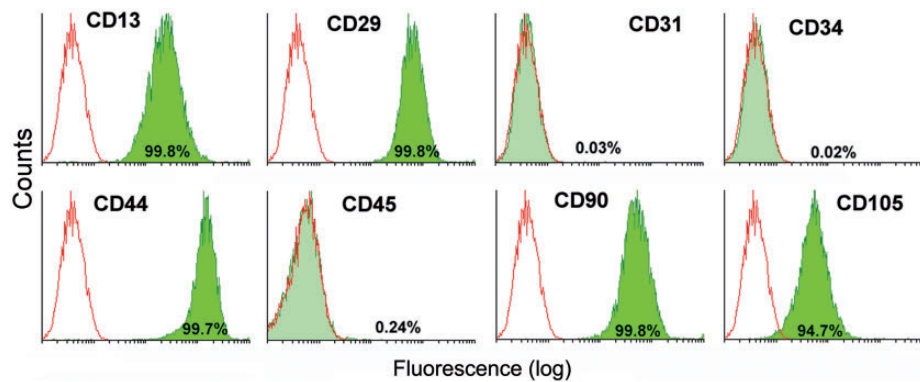


Figure 1 Analysis of stem cell-surface markers on UCMSCs. Expanded UCMSCs that were collected from two individuals and pooled were labeled with antibodies against cell surface antigens (CD13, CD29, CD44, CD90, CD31, CD34, CD45, and CD105) and analyzed via flow cytometry. Open histograms represent the background signal; the green histogram indicates a positive signal for the indicated antibody. The percentage listed depicts the percentage of cells that showed a positive signal above background for the indicated antibody. UCMSCs: umbilical cord mesenchymal stem cells. (A color version of this figure is available in the online journal.)

Repeated measures two-way ANOVA indicated significant differences ($P < 0.05$) in the gene expression of *PPAR γ* , *C/EBP α* , *FABP4*, *GPD1*, *PLIN1*, *PLIN2*, and *ADIPOQ* between groups at every time point following two weeks of differentiation (Figure 2a). For all genes, MDI-I and MDI-R induced significantly greater gene expression than did treatment with MDI alone ($P < 0.05$). By five weeks, gene expression in cells differentiated with MDI-I was significantly greater than in cells differentiated with MDI or MDI-R for all genes ($P < 0.001$), with the exception of leptin where MDI-R induced the greatest expression (Figure 2a). Interestingly, UCMSCs differentiated in MDI-R had significantly greater mRNA expression of *FABP4* ($P < 0.001$) and *PLIN1* ($P < 0.001$) compared to MDI and MDI-I at two weeks of differentiation. Thereafter, a decrease or leveling off in gene expression for many of the adipogenic genes occurred in the MDI-R group.

To confirm that the changes in mRNA expression of adipogenic genes with varying differentiation conditions were not unique to the initial UCMSC samples, additional UCMSCs were isolated ($N=4$) and differentiated as described earlier. Total RNA was isolated at 0, 2, and 5 weeks after adipogenic differentiation and real-time PCR analysis of adipogenic differentiation genes was performed (Figure 2b). Similar to the results from initial time course studies, experiments with biological replicates also showed that at five weeks following differentiation, cells treated with MDI-I showed greater extent of differentiation as seen by enhanced expression of *PPAR γ* , *C/EBP α* , *GPD1*, and *PLIN1* compared to those differentiated with MDI or MDI-R.

TG accumulation in lipid droplets is indicative of a mature adipocyte and increases throughout the differentiation process. Therefore, the amount of TG present is a common way of measuring the degree of adipocyte differentiation. To measure TG accumulation, we performed semi-quantitative analysis of Oil-red-O stained UCMSCs differentiated in MDI, MDI-I, or MDI-R. Consistent with gene expression changes, lipid staining was apparent in nearly all cells treated with MDI, MDI-I, and MDI-R by

one week (Figure 3a) and progressively increased over the five weeks in both MDI and MDI-I treated cells (Figure 3b). Similar to what was observed with gene expression, cells treated with MDI-R had a drop in lipid staining between two weeks and three weeks, after which TG storage increased to similar levels as those observed at one week post treatment, suggesting a potential loss of differentiation or differentiated cells. Repeated measures two-way ANOVA showed that after three weeks of treatment, cells differentiated in MDI-I had significantly more TG compared to either MDI or MDI-R. As differentiation progresses, adipocytes not only accumulate greater amounts of TG, but they also display larger lipid droplets. To semi-quantitatively measure lipid droplet size, we divided the total area of Oil-red-O staining by the number of particles measured. Interestingly at two weeks, cells differentiated in MDI-R had significantly larger lipid droplets compared to MDI and MDI-I (Figure 3c), which dramatically decreased by three weeks and was no longer different than MDI or MDI-I. By five weeks of differentiation, MDI-I had both more TG accumulation (Figure 3b) and significantly larger lipid droplets (Figure 3c) than both MDI and MDI-R, suggesting that MDI-I had the most potent effect on adipocyte differentiation.

MDI-I drives adipogenesis by increasing C/EBP α

Next we measured protein levels of *PPAR γ* and *C/EBP α* to ascertain if protein level changes paralleled the observed gene expression changes (Figure 4a). Following two and five weeks of differentiation, *PPAR γ* protein levels were significantly increased by at least 1.5-fold and 2.5-fold, respectively (Figure 4b), in all groups when compared to undifferentiated UCMSCs. However, in contrast to gene expression changes, there were no significant differences in *PPAR γ* protein levels between MDI, MDI-I, or MDI-R groups after five weeks of differentiation (Figure 4b). On the other hand, *C/EBP α* protein levels were more consistent with the observed gene expression changes (Figure 4a, c). Accordingly, MDI-I treatment induced the greatest increase in *C/EBP α* protein expression by two and five weeks

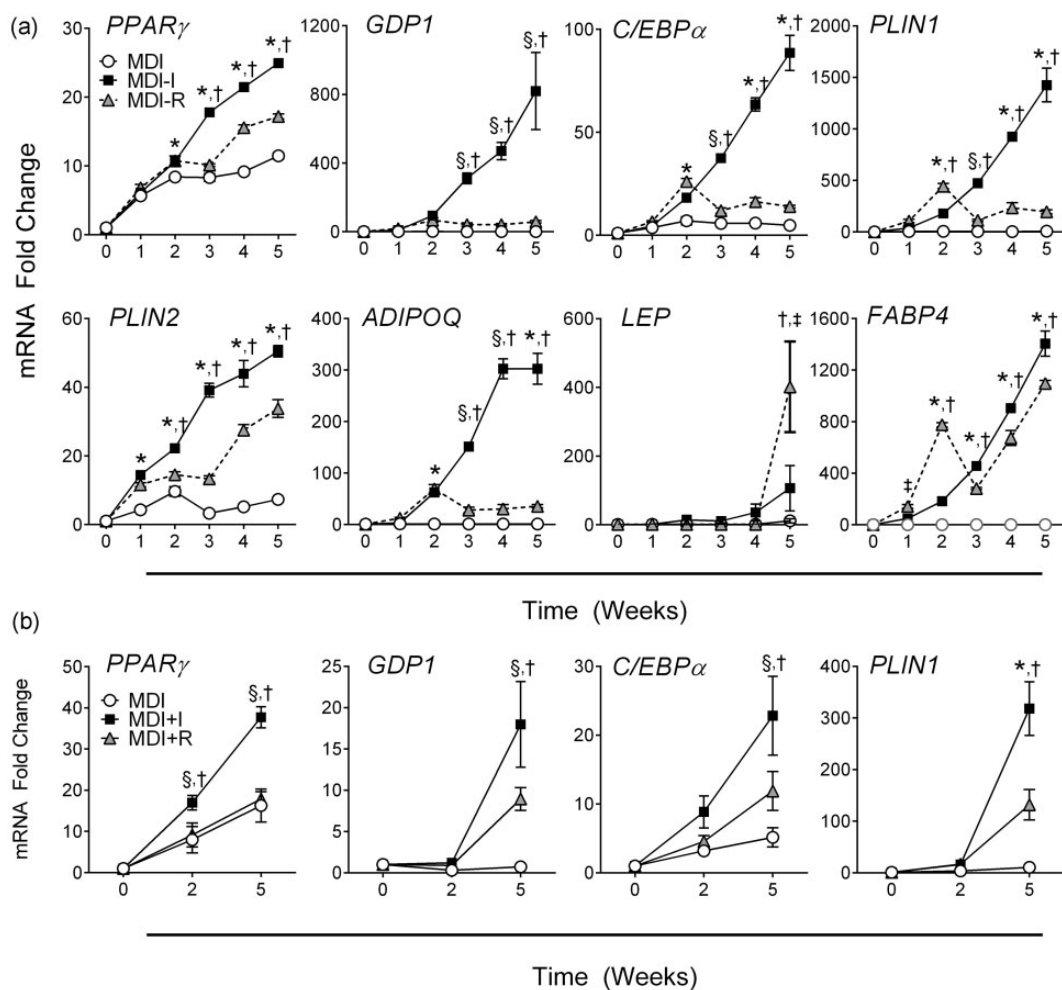


Figure 2 Time course analysis of adipogenic gene expression following differentiation. (a) The time course of mRNA expression in UCMSCs differentiated with MDI (open circle), MDI-I (black square), and MDI-R (gray triangle) for 0–5 weeks was analyzed via quantitative RT-PCR (*n* = 6 replicates per treatment group). (b) Changes in mRNA expression of adipogenic genes in UCMSCs differentiated with MDI (open circle), MDI-I (black square), and MDI-R (gray triangle) were confirmed in biological UCMSC replicates (*N* = 4) at 0, 2, and 5 weeks. Values are expressed as mean fold change from undifferentiated UCMSCs (0 week) \pm SE. Repeated measures two-way ANOVA followed by Tukey's multiple comparison test was performed to compare treatment groups. For each time point, * represents a significant difference from MDI, † represents a significant difference between MDI-I and MDI-R, ‡ represents a significant difference between MDI and MDI-R, and § represents a significant difference between MDI and MDI-I (*P* < 0.05). UCMSCs: umbilical cord mesenchymal stem cells

(3-fold and 6-fold, respectively), whereas there was no significant effect of MDI or MDI-R on *C/EBP α* levels by five weeks (Figure 4c). These data suggest that indomethacin may drive the expression of *C/EBP α* independently of other adipogenic stimuli. *C/EBP α* plays a significant role in regulating the genetic program that synchronizes adipogenesis and may therefore be the underlying mechanism for which MDI-I has such potent effects on adipocyte differentiation. To test if indomethacin could directly induce *C/EBP α* levels, we cultured UCMSCs for 0, 1, and 3 days in DMEM supplemented with 10% FBS and 60 μ M indomethacin and measured protein levels of *C/EBP α* and its upstream regulator *C/EBP β* (Figure 5). Following one day of indomethacin treatment, we observed a 1.8-fold increase in the amount of *C/EBP β* protein but no increase in *C/EBP α* . By three days of treatment there was a significant increase in both *C/EBP β* (2-fold) and *C/EBP α*

(1.5-fold) compared to untreated UCMSCs indicating that indomethacin can induce *C/EBP α* protein in absence of MDI, most likely through stimulation of *C/EBP β* expression.

Commitment with BMP4 stimulation

Because UCMSCs treated with MDI showed the least amount of differentiation, we next tested the hypothesis that akin to the mouse clonal MSC cell line C3H10T1/2, commitment to an adipocyte lineage via BMP4 stimulation (a known regulator of adipocyte commitment³⁵) would increase the response of UCMSCs to MDI-induced differentiation (Figure 6). Treatment with 50, 100, or 150 ng/mL of BMP4 for four days significantly increased mRNA expression of *ZFP423* and decreased expression of *WISP2* (Wnt1 signaling pathway protein) in UCMSCs, however, there was

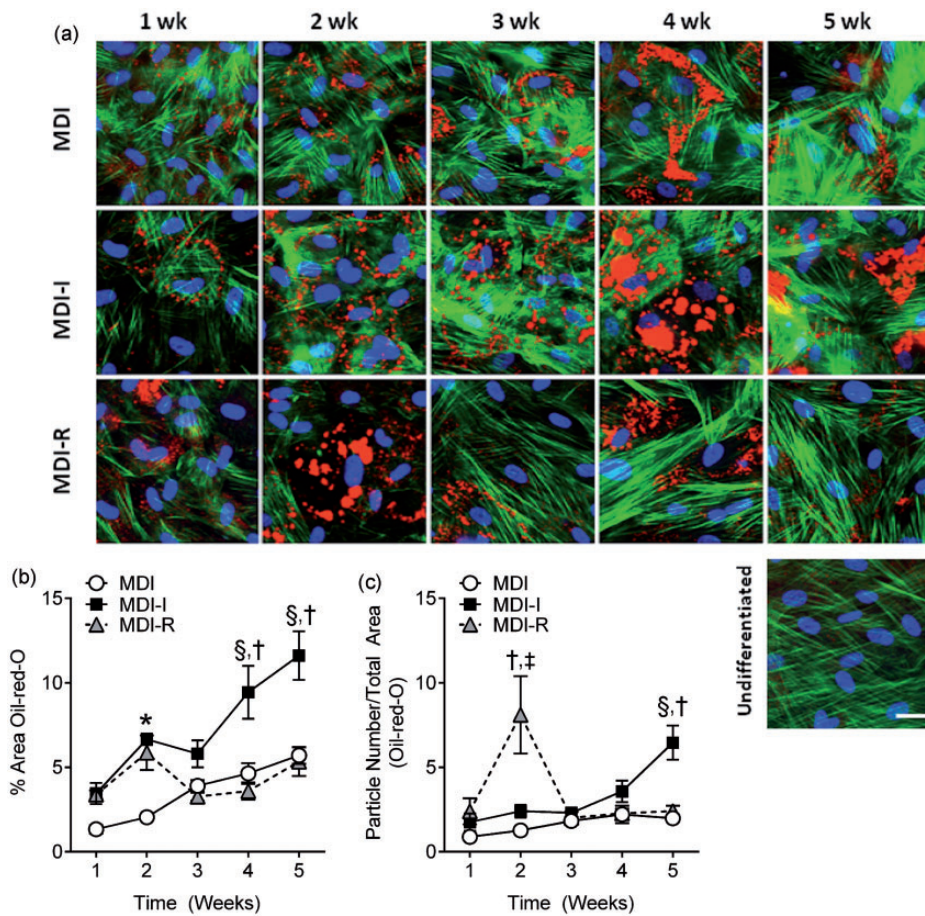


Figure 3 Semi-quantitative analysis of triglyceride accumulation and lipid droplet size in differentiated UCMSCs. UCMSCs differentiated for 1–5 weeks in MDI (open circle), MDI-I (black square), and MDI-R (gray triangle) were fixed and stained for neutral lipids with Oil-red-O (red), actin filaments with phalloidin (green), and DNA with DAPI (blue). The white calibration bar indicates 10 μ m. (a) Representative images of differentiated UCMSCs were taken at 40x using fluorescent microscopy. (b and c) Masking software (Axiovision) was used to quantify the areas stained red from 4–6 images per group, per time point. (b) Triglyceride accumulation was determined as the % area stained red normalized to the number of nuclei per image. (c) Lipid droplet size was determined by dividing the total masked area (red) by the number of particles counted. Values are expressed as mean \pm SE. Repeated measures two-way ANOVA with Tukey's *post hoc* test was performed to compare treatment groups. For each time point, * represents a significant difference between MDI and both MDI-I and MDI-R, † represents a significant difference between MDI-I and MDI-R, ‡ represents a significant difference between MDI and MDI-R, and § represents a significant difference between MDI and MDI-I ($P < 0.05$). DAPI: 4',6-diamidino-2-phenylindole; UCMSCs: umbilical cord mesenchymal stem cells. (A color version of this figure is available in the online journal.)

no dose-dependent response to BMP4 treatment (Figure 6a). Pre-treatment with 100 ng/mL of BMP4 showed a trend for increased TG storage in UCMSCs differentiated in MDI by one week, however there was no effect on UCMSCs differentiated in MDI-I or MDI-R (Figure 6b, c). By five weeks of differentiation, there was no effect of BMP4 treatment on TG storage for any of the groups (Figure 6c).

In cells pre-treated with BMP4 and differentiated for one week in MDI, there was no induction of *PPAR γ* , *C/EBP α* , or *FABP4* mRNA expression (Figure 6d). BMP4 pre-treated cells differentiated in MDI-I for one week also had no induction of *PPAR γ* , *C/EBP α* , or *FABP4* mRNA expression compared to control (Figure 6d). By five weeks of differentiation, BMP4-treated cells differentiated in MDI-R showed significantly reduced expressions of *PPAR γ* and *FABP4* compared to CON. BMP4 treatment led to significantly greater *PPAR γ* , *C/EBP α* , and *FABP4* gene expression by five weeks of differentiation in MDI-I compared to CON (Figure 6d).

Differentiated UCMSCs are insulin responsive at two weeks and resistant by five weeks

To test if differentiated UCMSCs were insulin responsive, we stimulated cells with 100 nmol/L insulin or vehicle at two or five weeks post differentiation and measured total and phosphorylated protein levels of AKT, ERK1/2, and JNK (Figure 7a). Following two weeks of differentiation, insulin stimulated a significant increase in ratio of phosphorylated AKT (P-AKT) to total AKT in cells treated with MDI, MDI-I, and MDI-R (Figure 7b), suggesting that these cells were insulin sensitive. Cells differentiated in MDI-I had a five-fold induction of P-AKT to AKT, compared to a 2-fold or a 1.7-fold increase in MDI or MDI-R treated cells, respectively, in response to the insulin challenge, suggesting that UCMSCs differentiated in MDI-I are the most insulin responsive. By five weeks of differentiation, only the cells treated with MDI had a significantly increased P-AKT/AKT ratio (Figure 7b) in response to

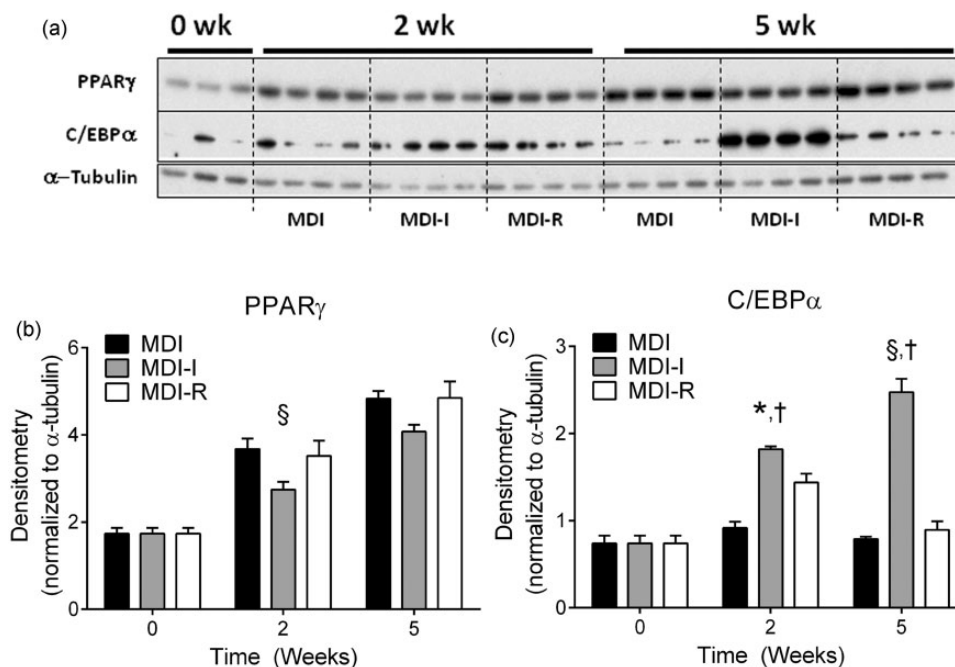


Figure 4 Analysis of PPAR γ and C/EBP α protein levels following two and five weeks of adipocyte differentiation. Protein levels of PPAR γ and C/EBP α in UCMSCs differentiated in MDI, MDI-I, and MDI-R for two and five weeks were analyzed via immunoblotting. (a) Immunoblots probed for PPAR γ and C/EBP α . (b and c) Densitometric analysis of PPAR γ and C/EBP α levels normalized to α -tubulin. Values are expressed as mean \pm SE. Significance between groups was determined using a repeated measures two-way ANOVA, followed by Tukey's multiple comparisons test. For each time point, * represents a significant difference between MDI and both MDI-I and MDI-R, † represents a significant difference between MDI-I and MDI-R, ‡ represents a significant difference between MDI and MDI-R, and § represents a significant difference between MDI and MDI-I ($P < 0.05$). C/EBP α : CCAAT-enhancer binding protein alpha; PPAR γ : peroxisome proliferator-activated receptor gamma; UCMSCs: umbilical cord mesenchymal stem cells

insulin, suggesting that long-term exposure to MDI-I and MDI-R may induce insulin resistance in UCMSCs.

Mitogen-activated protein kinases (MAPKs), ERK1/2 and JNK are also insulin responsive and become phosphorylated following insulin stimulation.^{38,39} Interestingly, the ratio of P-ERK1/2 to ERK1/2 was not significantly increased in response to insulin for any of the time points or groups, suggesting that ERK1/2 signaling is not insulin responsive in UCMSCs (Figure 7c). Insulin significantly increased the ratio of P-JNK to JNK in cells differentiated for two weeks in MDI and MDI-R by ~ 1.7 -fold (Figure 7d). However, by five weeks of differentiation, insulin stimulation lead to a significant decrease in JNK activation in the MDI and MDI-R groups. Interestingly, there was no effect of insulin on JNK activation in cells differentiated with MDI-I at either two or five weeks (Figure 7d).

Discussion

A number of cell culture models have been used to study the mechanisms regulating adipocyte differentiation. The UC is a recently identified source of MSCs that have adipogenic potential.^{7,26-28,40,41} As a novel source of fetal cells, UCMSCs can be used to determine if the *in utero* environment affects the differentiation potential of fetal stem cells. However, discrepancies exist regarding the techniques used to study *in vitro* adipogenic differentiation of these cells.^{25,42} Furthermore, their functional characterization as

adipocytes and cellular commitment to the adipocyte lineage has not been described. In this study, we tested the potential of three adipogenic cocktails used to stimulate adipocyte differentiation in UCMSCs and found that all three induced adipocyte differentiation, *albeit* to different levels. MDI-I was the most effective in inducing adipocyte differentiation and our data suggest that indomethacin-dependent regulation of C/EBP β and C/EBP α may be an underlying mechanism for the potent effects of MDI-I on UCMSC adipogenesis. Additionally, the present findings suggest that UCMSCs show minimal adipocyte differentiation in the absence of a PPAR γ ligand (MDI-treated), which cannot be rescued by BMP4-induced commitment. Finally, to our knowledge, we are the first to show that differentiated UCMSCs are insulin responsive early in differentiation but have decreased insulin sensitivity by five weeks of differentiation.

Cellular commitment to an adipocyte lineage is the first step in adipogenesis, followed by terminal differentiation.⁴³ In cells that have bipotential to differentiate into osteoblasts or adipocytes and in committed pre-adipocytes such as 3T3-L1 cells, MDI is a potent inducer of adipogenesis.⁴⁴ However, MDI alone is not sufficient to induce adipocyte differentiation in multipotent MSCs,⁴⁵ suggesting that some level of adipocyte commitment is necessary for MDI-induced adipogenesis. BMP4 is a member of the TGF β superfamily that promotes commitment of MSCs to an adipocyte lineage⁴⁵⁻⁴⁷ through regulating Wnt (wingless-type

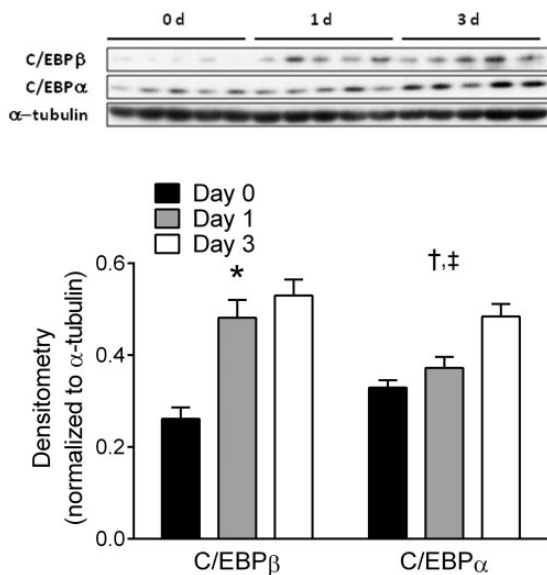


Figure 5 Analysis of C/EBP α and C/EBP β protein levels following 0, 1, and 3 days exposure to indomethacin. Protein levels of C/EBP α and C/EBP β in UCMSCs treated with 60 μ mol/L indomethacin for 0 (black bar), 1 (gray bar), and 3 (white bar) days were analyzed via immunoblot analysis. The graph depicts densitometric quantitation of immunoblots probed for C/EBP α and C/EBP β . Values are expressed as mean \pm SE. Significance between groups was determined using a repeated measures two-way ANOVA, followed by Tukey's test for multiple comparisons. For each time point, * represents a significant difference between MDI and both MDI-I and MDI-R, † represents a significant difference between MDI-I and MDI-R, ‡ represents a significant difference between MDI and MDI-R, and § represents a significant difference between MDI and MDI-I ($P < 0.05$). C/EBP α : CCAAT-enhancer binding protein alpha; UCMSCs: umbilical cord mesenchymal stem cells

MMTV integration site family) signaling. Specifically, BMP4 induces the dissociation of Zfp423 from WISP2⁴⁶ leading to nuclear translocation of Zfp423 and increased PPAR γ expression.⁴⁸ Zfp423 is elevated in preadipocyte cell lines and regulates basal levels of PPAR γ , suggesting that it may be a marker for adipocyte commitment.⁴⁸ We observed submaximal differentiation of UCMSCs in the presence of MDI, suggesting that these cells may need some prior adipocyte commitment stimulation. However, BMP4 treatment had minimal effects on increasing the responsiveness of UCMSCs to MDI. While BMP4 stimulation increased Zfp423 and decreased WISP2 gene expression, there was very little effect of BMP4 on lipid accumulation or gene expression following differentiation. Untreated UCMSCs had a relatively high basal level of PPAR γ protein and small amounts of lipid accumulation, suggesting that these cells may already be primed for adipocyte commitment. It is possible that a component of the UCMSC growth media induced a preadipocyte competency, making these cells more receptive to adipocyte differentiation.

In C3H10T1/2 pluripotent stem cells, MDI-I induces PPAR γ expression,³¹ therefore it was not surprising that in our UCMSCs, MDI-I had the greatest effects on adipocyte differentiation. However, differences between the effects of MDI-I and MDI-R on UCMSC adipogenesis were not anticipated because both indomethacin and rosiglitazone are

PPAR γ agonists. PPAR γ does not work alone in regulating the adipogenic program, C/EBP α also plays a significant role^{49,50} and C/EBP α and PPAR γ work in concert to regulate terminal differentiation of adipocytes by increasing the expression of each other and of key genes regulating adipocyte functions.^{24,51} Because PPAR γ protein levels did not differ between groups of UCMSCs, indomethacin- or rosiglitazone-stimulated PPAR γ expression cannot explain the phenotypic differences observed in differentiated UCMSCs. Thus, MDI-I-induced expression of C/EBP α may be driving increased differentiation of UCMSCs treated with MDI-I.

Obesity is often accompanied with hyperinsulinemia and insulin resistance of adipose, liver, and muscle tissues. Chronic insulin treatment in differentiated 3T3-L1 cells induces an insulin resistant state that is characterized by impaired PI3-kinase and MAP-kinase signaling.⁵² To our knowledge, this is the first report testing the insulin responsiveness of UCMSCs differentiated into adipocytes. Although the UCMSCs showed significant activation of AKT following insulin stimulation by two weeks of differentiation, by five weeks only the cells differentiated with MDI retained insulin sensitivity. These results are surprising, especially since thiazolidinediones, such as rosiglitazone, are insulin sensitizers. Additionally, C/EBP α , which is most elevated in the MDI-I group, is essential for maintaining insulin responsiveness.⁵³ Increased oxidative stress, ER stress, and mitochondrial dysfunction have all been implicated as potential mechanisms underlying the insulin resistance developed from chronic insulin exposure in 3T3-L1 cells.⁵⁴ Accordingly, indomethacin has been shown to induce oxidative stress and mitochondrial dysfunction in intestinal cells,⁵⁵ suggesting a potential mechanism for reduced insulin sensitivity in MDI-I differentiated UCMSCs. Alternatively, a more recent report indicates that a certain level of reactive oxygen species (ROS) production is necessary for adipogenesis to take place⁵⁶ and perhaps part of the potency of indomethacin as a inducer of adipogenesis is through stimulating ROS production.

Besides its role in regulating glucose uptake, insulin is also responsible for regulating a number of other metabolic and mitogenic pathways. ERK1/2 is a key mediator of the mitogenic actions of insulin⁵⁷ and is important for the insulin effects on adipocyte differentiation,⁵⁸ while JNK activation can induce insulin resistance⁵⁹⁻⁶¹ by inhibiting insulin signaling. Interestingly, although ERK1/2 activation increased over time with adipocyte differentiation, UCMSCs did not respond to insulin by activating ERK1/2, suggesting that this mitogenic pathway was inactive. We observed the activation of JNK in response to insulin stimulation earlier during differentiation, however this was reversed by five weeks.

In conclusion, the present studies uncover fundamental aspects of UCMSC differentiation capacity towards the adipocytic lineage. Our findings clearly demonstrate that while all three conditions promote adipocyte differentiation, MDI-I was the most effective at inducing adipocyte differentiation. These findings are consistent with indomethacin-dependent regulation of C/EBP β and C/EBP α

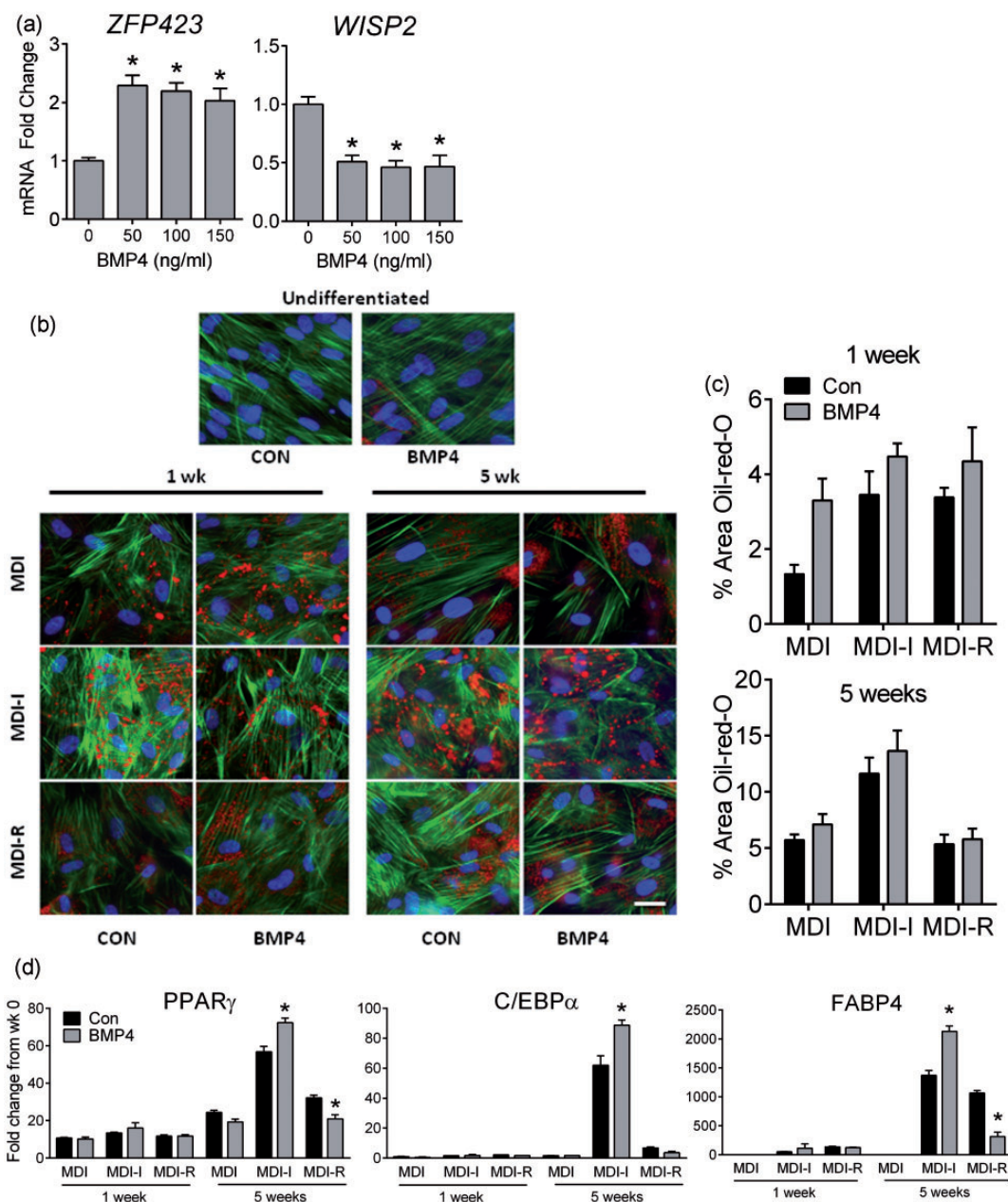


Figure 6 Analysis of adipocyte commitment in UCMSCs via BMP4 stimulation. UCMSCs were treated with or without BMP4 for four days prior to differentiation with MDI, MDI-I, MDI +R. (a) Quantitative RT-PCR analysis of *WISP2* and *ZFP423* mRNA expressions in UCMSCs following increasing doses (50, 100, 150 ng/mL) of BMP4. Values are expressed as the mean fold change from untreated cells (0) \pm SE. Significance between 0 and 50, 100, or 150 was determined using one-way ANOVA, followed by Tukey's *post hoc* test (*represents a significant difference from untreated cells, $P < 0.05$). (b) Representative, 40 \times images of UCMSCs treated with (CON) or without BMP4 (100 ng/mL) following adipocyte differentiation for one and five weeks. Triglyceride = red (Oil-red-O stain), Actin = green (phalloidin stain), Nuclei = blue (DAPI stain). The white calibration bar indicates 10 μ m. (c) Semi-quantitative analysis of triglyceride accumulation using masking software (Axiovision) as described in 'Methods' section. Values are expressed as mean % area \pm SE following normalization to number of nuclei. A repeated measures two-way ANOVA was used to compare CON (black bar) and BMP4 (gray bar) groups for cells differentiated with MDI, MDI-I, or MDI-R ($P < 0.05$). (d) Quantitative RT-PCR analysis of *PPAR γ* , *C/EBP α* , and *FABP4* mRNA expressions in UCMSCs treated with (CON) or without BMP4 (100 ng/mL) prior to differentiation. Values are expressed as the mean fold change from untreated cells (0 week) \pm SE. Significant differences were determined by repeated measures two-way ANOVA followed by Sidak's multiple comparisons test. * Represents a significant difference ($P < 0.05$) between CON (black bars) and BMP4 (gray bars) at each time point under the varying differentiation conditions (MDI, MDI-I, or MDI-R) ($P < 0.05$). BMP4: bone morphogenetic protein 4; DAPI: 4',6-diamidino-2-phenylindole; UCMSCs: umbilical cord mesenchymal stem cells; *WISP2*: Wnt1 signaling pathway protein 2. (A color version of this figure is available in the online journal.)

as an underlying mechanism for the potent effects of MDI-I on UCMSC adipogenesis. Importantly, the present findings also suggest that UCMSCs demonstrate minimal adipocyte differentiation in the absence of a *PPAR γ* ligand (MDI-alone), which cannot be rescued by BMP4-induced commitment. Finally, these studies reveal that *ex vivo*

differentiated UCMSCs are insulin responsive early in differentiation but have decreased sensitivity by five weeks of differentiation. Overall, these data provide primary evidence relating to the functional capacity of *ex vivo* differentiated UCMSC-derived adipocytes and their adipogenic potential.

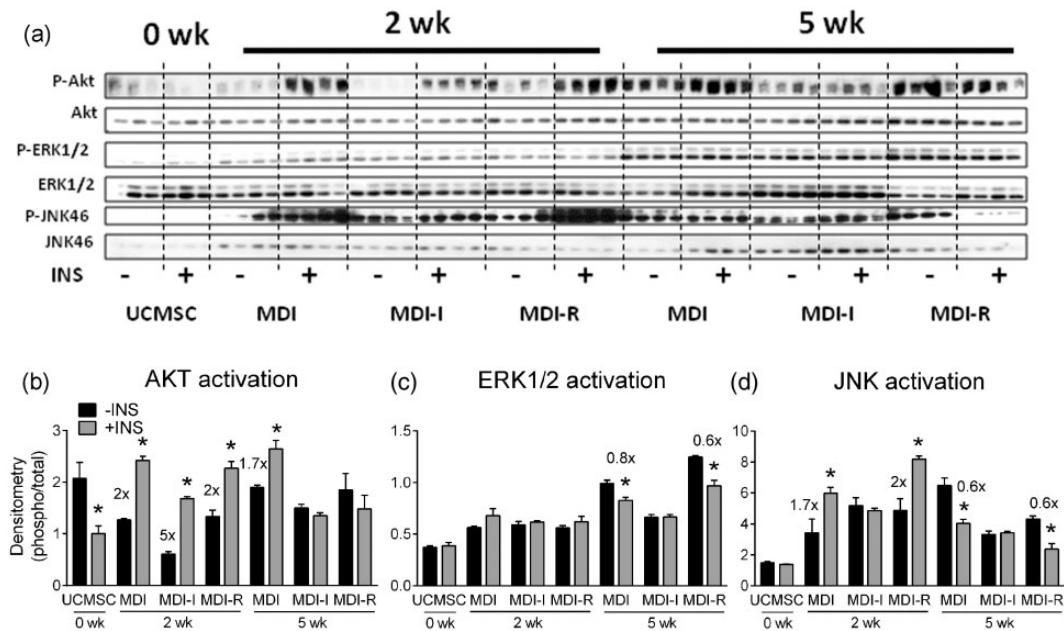


Figure 7 Analysis of AKT, ERK1/2, and JNK activation in differentiated UCMSCs following insulin challenge. UCMSCs differentiated with MDI, MDI-I, or MDI-R for two and five weeks were serum starved overnight and stimulated with (+INS) or without (–INS) 100 nmol/L insulin for 10 min. Protein levels of phosphorylated (P–) and total AKT, ERK1/2, and JNK were analyzed via immunoblotting. (a) Images of immunoblots probed for P-AKT, AKT, P-ERK1/2, ERK1/2, P-JNK, JNK, and α -tubulin. Densitometric analysis of (b) AKT, (c) ERK1/2, and (d) JNK levels normalized to α -tubulin. Values are expressed as the mean ratio of phosphorylated to total protein \pm SE. Significant differences were determined by repeated measures two-way ANOVA followed by Sidak's multiple comparisons test. * Represents a significant difference ($P < 0.05$) between –INS (black bar) and +INS (gray bar) at each time point under the varying differentiation conditions (MDI, MDI-I, or MDI-R). UCMSCs: umbilical cord mesenchymal stem cells

Author contributions: JS, AA, TMB, and KS conceived and designed the study; JS, FEL, and YZ performed laboratory experiments; JS, KMT, AA, KS, and TMB analyzed data and interpreted the results; JS created the figures and drafted the manuscript; JS, KMT, KS, AA, and TMB edited and revised manuscript; all authors approved the final version of the manuscript.

ACKNOWLEDGMENTS

We thank the members of the ACNC-Human Studies Core for their assistance. These studies were supported in part by the U.S. Department of Agriculture-ARS-CRIS 6251-51000-005-00D and National Institutes for Health Grant R01-DK084225 (K.S.). Nursing support was provided in part by the UAMS Translational Research Institute funded by the NIH-CTSA program, Grants UL1-TR-000039 and KL2-TR-000063.

REFERENCES

- Tsagias N, Koliakos I, Karagiannis V, Eleftheriadou M, Koliakos GG. Isolation of mesenchymal stem cells using the total length of umbilical cord for transplantation purposes. *Transfus Med* 2011;**21**:253–61
- Weiss ML, Medicetty S, Bledsoe AR, Rachakatla RS, Choi M, Merchav S, Luo Y, Rao MS, Velagaleti G, Troyer D. Human umbilical cord matrix stem cells: preliminary characterization and effect of transplantation in a rodent model of Parkinson's disease. *Stem Cells* 2006;**24**:781–92
- Yan M, Sun M, Zhou Y, Wang W, He Z, Tang D, Lu S, Wang X, Li S, Li H. Conversion of human umbilical cord mesenchymal stem cells in Wharton's jelly to dopamine neurons mediated by the Lmx1a and neurturin in vitro: potential therapeutic application for Parkinson's disease in a rhesus monkey model. *PLoS One* 2013;**8**:e64000
- Nekanti U, Mohanty L, Venugopal P, Balasubramanian S, Totey S, Ta M. Optimization and scale-up of Wharton's jelly-derived mesenchymal stem cells for clinical applications. *Stem Cell Res* 2010;**5**:244–254
- Nekanti U, Rao VB, Bahirvani AG, Jan M, Totey S, Ta M. Long-term expansion and pluripotent marker array analysis of Wharton's jelly-derived mesenchymal stem cells. *Stem Cells Dev* 2010;**19**:117–30
- Han Y, Chai J, Sun T, Li D, Tao R. Differentiation of human umbilical cord mesenchymal stem cells into dermal fibroblasts in vitro. *Biochem Biophys Res Commun* 2011;**413**:561–5
- Karahuseyinoglu S, Cinar O, Kilic E, Kara F, Akay GG, Demiralp DO, Tukun A, Uckan D, Can A. Biology of stem cells in human umbilical cord stroma: in situ and in vitro surveys. *Stem Cells* 2007;**25**:319–31
- Wang HS, Hung SC, Peng ST, Huang CC, Wei HM, Guo YJ, Fu YS, Lai MC, Chen CC. Mesenchymal stem cells in the Wharton's jelly of the human umbilical cord. *Stem Cells* 2004;**22**:1330–7
- Esposito M, Lucariello A, Costanzo C, Fiumarella A, Giannini A, Riccardi G, Riccio I. Differentiation of human umbilical cord-derived mesenchymal stem cells, WJ-MSCs, into chondrogenic cells in the presence of pulsed electromagnetic fields. *In Vivo* 2013;**27**:495–500
- Conconi MT, Burra P, Di Liddo R, Calore C, Turetta M, Bellini S, Bo P, Nussdorfer GG, Parnigotto PP. CD105(+) cells from Wharton's jelly show in vitro and in vivo myogenic differentiative potential. *Int J Mol Med* 2006;**18**:1089–96
- Zeddou M, Briquet A, Relic B, Josse C, Malaise MG, Gothot A, Lechanteur C, Beguin Y. The umbilical cord matrix is a better source of mesenchymal stem cells (MSC) than the umbilical cord blood. *Cell Biol Int* 2010;**34**:693–701
- Anzalone R, Lo Iacono M, Corrao S, Magno F, Loria T, Cappello F, Zummo G, Farina F, La Rocca G. New emerging potentials for human Wharton's jelly mesenchymal stem cells: immunological features and hepatocyte-like differentiative capacity. *Stem Cells Dev* 2010;**19**:423–38
- Ma L, Feng XY, Cui BL, Law F, Jiang XW, Yang LY, Xie QD, Huang TH. Human umbilical cord Wharton's Jelly-derived mesenchymal stem cells differentiation into nerve-like cells. *Chin Med J (Engl)* 118:1987–93

14. Mitchell KE, Weiss ML, Mitchell BM, Martin P, Davis D, Morales L, Helwig B, Beerstrauch M, Abou-Easa K, Hildreth T, Troyer D, Medicetty S. 2003 Matrix cells from Wharton's jelly form neurons and glia. *Stem Cells* 2005;**21**:50-60
15. Jo CH, Kim OS, Park EY, Kim BJ, Lee JH, Kang SB, Han HS, Rhee SH, Yoon KS. Fetal mesenchymal stem cells derived from human umbilical cord sustain primitive characteristics during extensive expansion. *Cell Tissue Res* 2008;**334**:423-33
16. Dorransoro A, Robbins PD. Regenerating the injured kidney with human umbilical cord mesenchymal stem cell-derived exosomes. *Stem Cell Res Ther* 2013;**4**:39
17. Li T, Yan Y, Wang B, Qian H, Zhang X, Shen L, Wang M, Zhou Y, Zhu W, Li W, Xu W. Exosomes derived from human umbilical cord mesenchymal stem cells alleviate liver fibrosis. *Stem Cells Dev* 2013;**22**:845-54
18. Bays HE, Gonzalez-Campoy JM, Bray GA, Kitabchi AE, Bergman DA, Schorr AB, Rodbard HW, Henry RR. Pathogenic potential of adipose tissue and metabolic consequences of adipocyte hypertrophy and increased visceral adiposity. *Expert Rev Cardiovasc Ther* 2008;**6**:343-68
19. Hoffstedt J, Arner E, Wahrenberg H, Andersson DP, Qvisth V, Lofgren P, Ryden M, Thorne A, Wiren M, Palmer M, Thorell A, Toft E, Arner P. Regional impact of adipose tissue morphology on the metabolic profile in morbid obesity. *Diabetologia* 2010;**53**:2496-503
20. Tang QQ, Lane MD. Adipogenesis: from stem cell to adipocyte. *Annu Rev Biochem* 2012;**81**:715-36
21. Cristancho AG, Lazar MA. Forming functional fat: a growing understanding of adipocyte differentiation. *Nat Rev Mol Cell Biol* 2011;**12**:722-34
22. Corneliu P, MacDougald OA, Lane MD. Regulation of adipocyte development. *Annu Rev Nutr* 1994;**14**:99-129
23. MacDougald OA, Lane MD. Transcriptional regulation of gene expression during adipocyte differentiation. *Annu Rev Biochem* 1995;**64**:345-73
24. Mandrup S, Lane MD. Regulating adipogenesis. *J Biol Chem* 1997;**272**:5367-70
25. Scott MA, Nguyen VT, Levi B, James AW. Current methods of adipogenic differentiation of mesenchymal stem cells. *Stem Cells Dev* 2011;**20**:1793-804
26. Peng KW, Liou YM. Differential role of actin-binding proteins in controlling the adipogenic differentiation of human CD105-positive Wharton's Jelly cells. *Biochim Biophys Acta* 2012;**1820**:469-81
27. Ragni E, Viganò M, Parazzi V, Montemurro T, Montelatici E, Lavazza C, Budelli S, Vecchini A, Rebullà P, Giordano R, Lazzari L. Adipogenic potential in human mesenchymal stem cells strictly depends on adult or foetal tissue harvest. *Int J Biochem Cell Biol* 2013;**45**:2456-66
28. Kim DW, Staples M, Shinozuka K, Pantcheva P, Kang SD, Borlongan CV. Wharton's jelly-derived mesenchymal stem cells: phenotypic characterization and optimizing their therapeutic potential for clinical applications. *Int J Mol Sci* 2013;**14**:11692-712
29. Ciavarella S, Dammacco F, De Matteo M, Loverro G, Silvestris F. Umbilical cord mesenchymal stem cells: role of regulatory genes in their differentiation to osteoblasts. *Stem Cells Dev* 2009;**18**:1211-20
30. Rosen ED, Walkey CJ, Puigserver P, Spiegelman BM. Transcriptional regulation of adipogenesis. *Genes Dev* 2000;**14**:1293-307
31. Styner M, Sen B, Xie Z, Case N, Rubin J. Indomethacin promotes adipogenesis of mesenchymal stem cells through a cyclooxygenase independent mechanism. *J Cell Biochem* 2010;**111**:1042-50
32. Wang D, Haile A, Jones LC. Rosiglitazone-induced adipogenesis in a bone marrow mesenchymal stem cell line - biomed 2011. *Biomed Sci Instrum* 2011;**47**:213-21
33. Benvenuti S, Cellai I, Luciani P, Deledda C, Baglioni S, Giuliani C, Saccardi R, Mazzanti B, Dal Pozzo S, Mannucci E, Peri A, Serio M. Rosiglitazone stimulates adipogenesis and decreases osteoblastogenesis in human mesenchymal stem cells. *J Endocrinol Invest* 2007;**30**:RC26-30
34. Welters HJ, El Ouaamari A, Kawamori D, Meyer J, Hu J, Smith DM, Kulkarni RN. Rosiglitazone promotes PPARgamma-dependent and -independent alterations in gene expression in mouse islets. *Endocrinology* 2012;**153**:4593-9
35. Huang H, Song TJ, Li X, Hu L, He Q, Liu M, Lane MD, Tang QQ. BMP signaling pathway is required for commitment of C3H10T1/2 pluripotent stem cells to the adipocyte lineage. *Proc Natl Acad Sci U S A* 2009;**106**:12670-5
36. Seshareddy K, Troyer D, Weiss ML. Method to isolate mesenchymal-like cells from Wharton's Jelly of umbilical cord. *Methods Cell Biol* 2008;**86**:101-19
37. Saben J, Zhong Y, Gomez-Acevedo H, Thakali KM, Borengasser SJ, Andres A, Shankar K. Early growth response protein-1 mediates lipotoxicity-associated placental inflammation: role in maternal obesity. *Am J Physiol Endocrinol Metab* 2013;**305**:E1-14
38. Lazar DF, Wiese RJ, Brady MJ, Mastick CC, Waters SB, Yamauchi K, Pessin JE, Cuatrecasas P, Saltiel AR. Mitogen-activated protein kinase inhibition does not block the stimulation of glucose utilization by insulin. *J Biol Chem* 1995;**270**:20801-7
39. Lee YH, Giraud J, Davis RJ, White MF. c-Jun N-terminal kinase (JNK) mediates feedback inhibition of the insulin signaling cascade. *J Biol Chem* 2003;**278**:2896-902
40. Lu LL, Liu YJ, Yang SG, Zhao QJ, Wang X, Gong W, Han ZB, Xu ZS, Lu YX, Liu D, Chen ZZ, Han ZC. Isolation and characterization of human umbilical cord mesenchymal stem cells with hematopoiesis-supportive function and other potentials. *Haematologica* 2006;**91**:1017-26
41. Ciavarella S, Dammacco F, De Matteo M, Loverro G, Silvestris F. Umbilical cord mesenchymal stem cells: role of regulatory genes in their differentiation to osteoblasts. *Stem Cells Dev* 2009;**18**:1211-20
42. Bosch J, Houben AP, Radke TF, Stapelkamp D, Bunemann E, Balan P, Buchheiser A, Liedtke S, Kogler G. Distinct differentiation potential of "MSC" derived from cord blood and umbilical cord: are cord-derived cells true mesenchymal stromal cells? *Stem Cells Dev* 2012;**21**:1977-88
43. Bowers RR, Lane MD. Wnt signaling and adipocyte lineage commitment. *Cell Cycle* 2008;**7**:1191-6
44. Ding J, Nagai K, Woo JT. Insulin-dependent adipogenesis in stromal ST2 cells derived from murine bone marrow. *Biosci Biotechnol Biochem* 2003;**67**:314-21
45. Tang QQ, Otto TC, Lane MD. Commitment of C3H10T1/2 pluripotent stem cells to the adipocyte lineage. *Proc Natl Acad Sci U S A* 2004;**101**:9607-11
46. Hammarstedt A, Hedjazifar S, Jenndahl L, Gogg S, Grunberg J, Gustafson B, Klimcakova E, Stich V, Langin D, Laakso M, Smith U. WISP2 regulates preadipocyte commitment and PPARgamma activation by BMP4. *Proc Natl Acad Sci U S A* 2013;**110**:2563-8
47. Bowers RR, Kim JW, Otto TC, Lane MD. Stable stem cell commitment to the adipocyte lineage by inhibition of DNA methylation: role of the BMP-4 gene. *Proc Natl Acad Sci U S A* 2006;**103**:13022-7
48. Gupta RK, Arany Z, Seale P, Mepani RJ, Ye L, Conroe HM, Roby YA, Kulaga H, Reed RR, Spiegelman BM. Transcriptional control of preadipocyte determination by Zfp423. *Nature* 2010;**464**:619-23
49. Freytag SO, Paielli DL, Gilbert JD. Ectopic expression of the CCAAT/enhancer-binding protein alpha promotes the adipogenic program in a variety of mouse fibroblastic cells. *Genes Dev* 1994;**8**:1654-63
50. Lin FT, Lane MD. CCAAT/enhancer binding protein alpha is sufficient to initiate the 3T3-L1 adipocyte differentiation program. *Proc Natl Acad Sci U S A* 1994;**13**:8757-61
51. Rosen ED, Spiegelman BM. Molecular regulation of adipogenesis. *Annu Rev Cell Dev Biol* 2000;**16**:145-71
52. Ricort JM, Tanti JF, Van Obberghen E, Marchand-Brustel Y. Alterations in insulin signalling pathway induced by prolonged insulin treatment of 3T3-L1 adipocytes. *Diabetologia* 1995;**38**:1148-56
53. Wu Z, Rosen ED, Brun R, Hauser S, Adelmant G, Troy AE, McKeon C, Darlington GJ, Spiegelman BM. Cross-regulation of C/EBP alpha and PPAR gamma controls the transcriptional pathway of adipogenesis and insulin sensitivity. *Mol Cell* 1999;**3**:151-8
54. Ge X, Yu Q, Qi W, Shi X, Zhai Q. Chronic insulin treatment causes insulin resistance in 3T3-L1 adipocytes through oxidative stress. *Free Radic Res* 2008;**42**:582-91
55. Basivireddy J, Vasudevan A, Jacob M, Balasubramanian KA. Indomethacin-induced mitochondrial dysfunction and oxidative stress in villus enterocytes. *Biochem Pharmacol* 2002;**64**:339-49

56. Higuchi M, Dusing GJ, Peshavariya H, Jiang F, Hsiao ST, Chan EC, Liu GS. Differentiation of human adipose-derived stem cells into fat involves reactive oxygen species and Forkhead box O1 mediated upregulation of antioxidant enzymes. *Stem Cells Dev* 2013;**22**:878–88
57. Taniguchi CM, Emanuelli B, Kahn CR. Critical nodes in signalling pathways: insights into insulin action. *Nat Rev Mol Cell Biol* 2006;**7**:85–96
58. Porras A, Santos E. The insulin/Ras pathway of adipocytic differentiation of 3T3 L1 cells: dissociation between Raf-1 kinase and the MAPK/RSK cascade. *Int J Obes Relat Metab Disord* 1996;**20**:S43–51
59. Aguirre V, Uchida T, Yenush L, Davis R, White MF. The c-Jun NH(2)-terminal kinase promotes insulin resistance during association with insulin receptor substrate-1 and phosphorylation of Ser(307). *J Biol Chem* 2000;**275**:9047–54
60. Nguyen MT, Satoh H, Favelyukis S, Babendure JL, Imamura T, Sbodio JI, Zalevsky J, Dahiyat BI, Chi NW, Olefsky JM. JNK and tumor necrosis factor- α mediate free fatty acid-induced insulin resistance in 3T3-L1 adipocytes. *J Biol Chem* 2005;**280**:35361–71
61. Evans JL, Goldfine ID, Maddux BA, Grodsky GM. Are oxidative stress-activated signaling pathways mediators of insulin resistance and beta-cell dysfunction? *Diabetes* 2003;**52**:1–8

(Received December 2, 2013, Accepted May 13, 2014)